A Five-Bar Finger Mechanism Involving Redundant Actuators: Analysis and Its Applications

Byung-Ju Yi, *Member, IEEE*, Sang-Rok Oh, *Member, IEEE*, and Il Hong Suh, *Member, IEEE*

***Abstract*— Analysis and useful applications of redundant actuation are addressed in this work. A five-bar finger mechanism driven by redundant actuators is given as an illustrative example. It is shown that judicial choice of the location of one redundant actuator greatly enhances the load handling capacity of the system, when compared to those of minimum actuation and more than two redundant actuation, Also, methodologies for stiffness and motion frequency modulations via redundant actuation are investigated in this work. Internal load distribution associated with the stiffness and motion frequency modulations is further discussed. Specifically, the motion frequency of the system is modulated by employing inertial and the spring-like impedance properties created by internal loading. The motion frequency as well as the amplitude of oscillation can be actively adjusted during the motion, and the equilibrium position about which the vibration occurs can also be arbitrarily changed during the motion. Furthermore, using the stiffness modulation capability, a point-to-point motion can be accomplished by a progressive movement of equilibrium posture, which is termed as a virtual trajectory. To show the effectiveness of the proposed algorithms, several simulation results are illustrated.**

***Index Terms*—Finger, frequency modulation, internal loading, redundant actuation, stiffness control, virtual trajectory.**

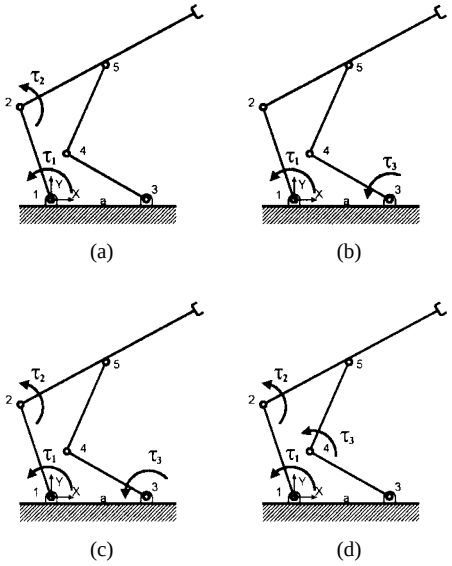

Fig. 1. Five-bar finger mechanisms.

I. Introduction

REDUNDANT actuation refers to the use of more actuators than the kinematic degree of freedom (or mobility) of a system. The abundance of potential input locations in structurally parallel mechanism or closed-chain linkage systems allows the implementation of redundant actuation (i.e., extra input drivers), which may be utilized for optimal load distribution [7]–[14] and beneficial internal load generation [15]–[26]. Moreover, redundant actuation admits fault-tolerant capability when some of the system actuators fail [27]. Such fault-tolerant capability of robot manipulators will be important in space operation and nuclear power plants where high reliability is vital.

Consider five-bar finger mechanisms given in Fig. 1. The five-bar requires at least two actuators to control the motion at the end-point. Fig. 1(a) and (b) denotes the case of minimum actuation. On the other hands, when this mechanism is driven by more than two actuators as seen in Fig. 1(c)–(e), it is said redundantly actuated. Since there exists five potential input locations, several combinations of input locations can be thought for each case. Here, the actuator location should be carefully decided to enhance the desired performance. General biomechanical systems including the human body as well as the bodies of mammals and insects are also redundantly actuated. Fig. 2 denotes an anthropomorphic robot having six human actuators (i.e, muscles) while it requires two inputs to control the motion at the operational space. Furthermore, the real human upper-extremity (arm) is known to have 29 human actuators [1]. It has been presumed by biomechanicians that the human body employs redundant actuation for optimal load distribution and beneficial internal load generation. Thus, Hogan [6] raised a question for the existence of those hyper-redundant actuators inherent in the human body. He explained the existence of the hyper-redundant muscles of the human body in terms of the spring-like impedance property; An effective spring-like impedance property can be modulated by antagonistic activation of hyper-redundant muscles. Fig. 3 represents a single joint antagonistically activated by two muscles, resulting in creating an effective stiffness about the joint. Inspired by those ideas stemming from the biomechanics research fields, Yi and Freeman [15], [20], [21] proposed a general methodology for actively adjustable springs, and

Manuscript received January 11, 1998; revised April 16, 1999. This paper was recommended for publication by Associate Editor W. R. Hamel and Editor S. Salcudean upon evaluation of the reviewers' comments. This work was supported in part by the Basic Research Program, KOSEF under Grant 961-1001-007-2 and by the Development of Human Robot System under the KIST 2000 Program.

B.-J. Yi and I. H. Suh are with Hanyang University, Ansan, Kyungki-Do 425-791, Korea.

S.-R. Oh is with the Intelligent System Control Research Center, Korea Institute of Science and Technology, Seoul 136-130, Korea.

Publisher Item Identifier S 1042-296X(99)10327-6.

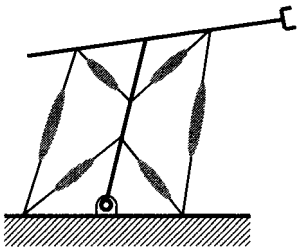

Fig. 2. Anthropomorphic robot.

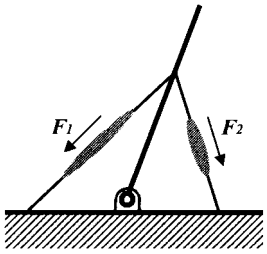

Fig. 3. Antagonistic activation.

conditions for actively adjustable springs are derived for general redundantly actuated closed-chain mechanisms.

Based on the motivation stated above, our work will be focused on useful applications of redundant actuation. The first objective is to provide a guideline of employing redundant actuation for the enhancement of the load handling capacity. The second objective is the beneficial application of excessive redundant actuation to generation of motion frequency. The feasibility of our proposed algorithms will be verified through a 5-bar finger mechanism with redundant actuators. We propose a five-bar mechanism as a finger mechanism which is equipped with compact joint-driven, redundant motors such as ultrasonic rotary actuators with high torque capacity. This configuration would be not only free from the friction effect occurring in tendon-driven methods, but also increase the payload of the finger due to redundant actuators as well as provide chances of applying several beneficial subtasks using internal loading.

In this work, we suggest that judicial choice of one additional redundant actuator greatly enhances the load handling capacity of the system, and that antagonistic activation of excessive redundant actuators enables the system to modulate the end-point motion frequency by internal load distributions. Using the frequency (or stiffness) modulation capability, we show that a point-to-point motion is accomplished by a progressive movement of equilibrium posture, which has been termed as a virtual trajectory by Hogan [6]. Especially, it is shown that using excessive redundant actuation, the motion frequency as well as the amplitude of oscillation can be actively adjusted during the motion, and that the equilibrium position about which the vibration occurs can be also arbitrarily altered during the motion.

The organization of this paper is as follows: Initially, we introduce kinematic and dynamic modeling methodology in Section II. In Section III, enhancement of maximum load handling capacity is shown to be possible when using redundant actuation. Stiffness and frequency modulation algorithm will be proposed in Section IV. Simulation results are included in Sections III and IV to corroborate our proposed concepts. Finally, we draw conclusions.

II. Kinematic Modeling

A. Definition

The modeling methodology integrates the Generalized Principle of D'Alembert with the method of kinematic influence coefficients (KIC) resulting in closed form vector expressions. The reader is referred to Freeman and Tesar [2] for a more detailed description. In the following, the letters G and H stand for 1st and 2nd order KIC matrices, respectively, and superscribed quantities located on the left-side of every parameters indicate dependent parameters while subscripts denote the independent parameters. Also, left subscriptions lying on the left-side of G and H represent the number of chain of multiple robot systems.

Let $[{}_rG^a_b]_{(i,j)}$ denote the (i,j)th element of Jacobian description $[{}_rG^a_b]$, and let $[{}_rG^a_b]_{(i,^*)}$ denote the ith row of $[{}_rG^a_b]$. And also $[{}_rG^a_b]_{(^*,i)}$ denote the ith column of $[{}_rG^a_b]$. Further, let $[{}_rH^a_{bb}]_{(i,j,k)}$ denote the (j,k)th element of the ith plane of the three-dimensional (3-D) array (Hessian description) $[{}_rH^a_{bb}]$. $[{}_rH^a_{bb}]_{(i,^*,^*)}$ implies the ith plane of the 3-D array $[{}_rH^a_{bb}]$, and so on [2].

B. Internal Kinematics for a Five-Bar Finger Mechanism

Consider a five-bar finger mechanism shown in Fig. 1. This system has two typical features. As the first feature, it has one closed-kinematic chain. The closed-kinematic chain is formed by connecting the two open-chains at the given location of the second link of the left open-chain, as shown in Fig. 1. In order to enlarge the area encompassed by the finger, the folded-in configuration of the right open-chain is chosen. As the second feature, there exist several choices in the selection of independent joints (i.e., actuator locations). Since the mobility of this mechanism is given as two, two actuators are minimally required to control the mechanism. In general, the base joints have been chosen as the actuator locations in previously developed 5-bar systems [5], primarily to minimize the dynamic effect due to floating actuators. However, from a kinematic point of view, inclusion of one or two floating actuators may be a better choice. For example, a better manipulability, isotropy, or load handling capacity can be achieved by using a certain floating actuator.

An internal kinematic relationship between the dependent joints and the independent joints is required to deal with our further analysis of the five-bar finger mechanism. Note that the two open-chain of the 5-bar finger mechanism have a common kinematic relation at the end-point of the system. Let the end-point vector of the 5-bar be denoted as $\mathbf{u} = (x\, y\, \Phi)^T$. Then, the components of $\boldsymbol{u}$ is written by [25]

$$x = l_1c_1 + l_2c_{12} = a + l_3c_3 + l_4c_{34} + l_5c_{345} \quad (1)$$

$$y = l_1s_1 + l_2s_{12} = l_3s_3 + l_4s_{34} + l_5s_{345} \quad (2)$$

and

$$\Phi = \theta_1 + \theta_2 = \theta_3 + \theta_4 + \theta_5. \tag{3}$$

Also, the equivalent velocity and acceleration relations are, respectively, given by

$$\dot{\boldsymbol{u}} = [{}_1G^u_\theta]{}_1\dot{\boldsymbol{\theta}} = [{}_2G^u_\theta]{}_2\dot{\boldsymbol{\theta}} \tag{4}$$

and

$$\begin{aligned}\ddot{\boldsymbol{u}} &= [{}_1G^u_\theta]{}_1\ddot{\boldsymbol{\theta}} + {}_1\dot{\boldsymbol{\theta}}^T[{}_1H^u_{\theta\theta}]{}_1\dot{\boldsymbol{\theta}} \\ &= [{}_2G^u_\theta]{}_2\ddot{\boldsymbol{\theta}} + {}_2\dot{\boldsymbol{\theta}}^T[{}_2H^u_{\theta\theta}]{}_2\dot{\boldsymbol{\theta}}\end{aligned} \tag{5}$$

where $[{}_1G^u_\theta]$ and $[{}_2G^u_\theta]$, respectively, imply the Jacobians of the first and second open-chain, and $[{}_1H^u_{\theta\theta}]$ and $[{}_2H^u_{\theta\theta}]$, respectively, denote the Hessian arrays of the first and second open-chain of the system.

Selecting the joints θ_1 and θ_2 as the independent joints (ϕ_a) and the joints θ_3, θ_4 and θ_5 as the dependent joints (ϕ_p), (4) can be rewritten as [3], [25]

$$\dot{\phi}_p = [G^p_a]\dot{\phi}_a \tag{6}$$

where

$$\dot{\phi}_p = \begin{pmatrix}\dot{\theta}_3 \\ \dot{\theta}_4 \\ \dot{\theta}_5\end{pmatrix} \tag{7}$$

$$\dot{\phi}_a = \begin{pmatrix}\dot{\theta}_1 \\ \dot{\theta}_2\end{pmatrix} \tag{8}$$

and $[G^p_a]_{3\times 2}$ denotes the first-order KIC matrix relating $\dot{\phi}_p$ to $\dot{\phi}_a$.

The second-order, 3-D KIC array $[H^p_{aa}]_{3\times 2\times 2}$ relating $\ddot{\phi}_p$ to $\ddot{\phi}_a$ and $\dot{\phi}_a$ can be easily obtained in a similar manner as follows [3]:

$$\ddot{\phi}_p = [G^p_a]\ddot{\phi}_a + \dot{\phi}^T_a[H^p_{aa}]\dot{\phi}_a. \tag{9}$$

Also $[H^\phi_{aa}]$ is defined as

$$[H^\phi_{aa}] = \begin{bmatrix}[0]_{2\times 2\times 2} \\ [H^p_{aa}]_{3\times 2\times 2}\end{bmatrix}_{5\times 2\times 2}. \tag{10}$$

According to the duality between the velocity vector and force vector, the force relation between the independent joints and the dependent joints is described by

$$\boldsymbol{T}_a = [G^p_a]^T\boldsymbol{T}_p \tag{11}$$

where

$$\begin{aligned}\boldsymbol{T}_a &= (T_1 \quad T_2)^T, \\ \boldsymbol{T}_p &= (T_3 \quad T_4 \quad T_5)^T.\end{aligned} \tag{12}$$

Then, when activating all the joint actuators, the effective load referenced to the independent joints is expressed by

$$\boldsymbol{T}^*_a = \boldsymbol{T}_a + [G^p_a]^T\boldsymbol{T}_p = [G^\phi_a]^T\boldsymbol{T}_\phi \tag{13}$$

where

$$[G^\phi_a]_{5\times 2} = \begin{bmatrix}[I]_{2\times 2} \\ [G^p_a]_{3\times 2}\end{bmatrix} \tag{14}$$

$$\boldsymbol{T}_\phi = (T_1 \quad T_2 \quad T_3 \quad T_4 \quad T_5)^T.$$

C. External Kinematics for Five-Bar Finger Mechanism

Since the joints of the rth chain are composed of some of independent and dependent joints, $({}_r\dot{\phi})$ can be expressed in terms of the total system's active (independent) joints by

$${}_r\dot{\phi} = [{}^rG^\phi_a]\hat{\phi}_a \tag{15}$$

where the matrix $[{}^rG^\phi_a]$ is formed using elements of $[G^p_a]$ augmented with a one in the ith row and jth column and with zeros in all other elements of the ith row if ${}_r\dot{\phi}_i = \dot{\phi}_{a_j}$. Thus, the external (or forward) kinematics for the common object is obtained by embedding the first-order KIC into one of the rth pseudo open-chain kinematic expressions as follows:

$$\dot{u} = [{}_rG^u_\phi]_r \quad \dot{\phi} = [G^u_a]\dot{\phi}_a \tag{16}$$

where the forward Jacobian is determined by

$$[G^u_a] = [{}_rG^u_\phi][{}_rG^\phi_a]. \tag{17}$$

Using the same augmentation method employed in (17), evaluation of the second-order kinematic array $[H^u_{aa}]$ is also straightforward. It is given by [3]

$$[H^u_{aa}] = [{}_rG^u_\phi]o[{}_rH^\phi_{aa}] + [{}_rG^\phi_a]^T[{}_rH^u_{\phi\phi}][{}_rG^\phi_a] \tag{18}$$

where "o" denotes a generalized scalar dot product (refer to Appendix 1 for the detailed description for this), and this description will be used in the stiffness model to be derived in Section IV.

D. Dynamic Modeling for Five-Bar Finger Mechanism

In this section, we introduce a dynamic model of the five-bar finger mechanism consisting of two open kinematic chains. Using the principle of virtual work, the generalized inertial loads of an M-link open-chain as referenced to the M relative joint parameters are given as [2]

$${}_r\mathbf{T}_\phi = [{}_rI^*_{\phi\phi}]_r\ddot{\phi} + {}_r\dot{\phi}^T[{}_rP^*_{\phi\phi\phi}]_r\dot{\phi}, \qquad (r = 1, 2) \tag{19}$$

where $[{}_rI^*_{\phi\phi}]$ and $[{}_rP^*_{\phi\phi\phi}]$ denote the effective inertia matrix and the inertia power array, respectively.

Now, employing the principle of virtual work, the open-chain dynamics can be directly incorporated into closed chain dynamics according to

$$\mathbf{T}^T_\phi\delta\phi = \mathbf{T}^T_a\delta\phi_a. \tag{20}$$

The total system dynamics is then obtained as follows:

$$\begin{aligned}\mathbf{T}^*_a &= [G^\phi_a]^T\boldsymbol{T}_\phi \\ &= [I^*_{aa}]\ddot{\phi}_a + \dot{\phi}^T_a[P^*_{aaa}]\dot{\phi}_a\end{aligned} \tag{21}$$

where the inertial matrix $[I^*_{aa}]$ and inertia power array $[P^*_{aaa}]$ defined in the independent joint set are given by [3]

$$[I^*_{aa}] = \sum_{r=1}^{2}[G^\phi_a]^T[{}_rI^*_{\phi\phi}][{}_rG^\phi_a], \tag{22}$$

$$\begin{aligned}[P^*_{aaa}] = \sum_{r=1}^{2}\{&([{}_rG^\phi_a]^T[{}_rI^*_{\phi\phi}]) \circ [{}_rH^\phi_{aa}] \\ &+ [{}_rG^\phi_o]^T([{}_rG^\phi_a]^T \circ [{}_rP^*_{\phi\phi\phi}])[{}_rG^\phi_a]\}\end{aligned} \tag{23}$$

and $[{}_rG_a^\phi]$ and $[{}_rH_{aa}^\phi]$, respectively, denote the first-order and the second-order kinematic influence coefficient matrices relating the joints of rth serial chain to the independent joints of the system.

Now, the dynamic formulation with respect to the output(task or operational) coordinates is obtained by employing the coordinate transformation technique between the minimum coordinates and the task coordinates [3]

$$\boldsymbol{T}_u = [I_{uu}^*]\ddot{\boldsymbol{u}} + \dot{\boldsymbol{u}}^T[P_{uuu}^*]\dot{\boldsymbol{u}} \tag{24}$$

where

$$[I_{uu}] = [G_u^a]^T[I_{aa}][G_u^a], \tag{25}$$

$$[P_{uuu}] = [G_u^a]^T([G_u^a]^T \circ [P_{aaa}])[G_u^a] + ([G_u^a]^T[I_{aa}]) \circ [H_{uu}^a] \tag{26}$$

and $\boldsymbol{T}_u$ denotes the load vector at the output position, and $[I_{uu}^*]$ and $[P_{uuu}^*]$ present the inertial matrix and inertia power array defined in the output position, respectively.

III. Analysis on Maximum Load Handling Capacity

A. Maximum Load Handling Capacity of a Five-Bar Finger Mechanism

Maximum load handling capacity is defined as the maximum load that can be applied to the end-effector in any direction without exceeding any one actuator limit.

Methodology to be described in the following is based on Thomas *et al.* [4]. We extend their algorithm to the case with redundant actuation. When a given closed-chain mechanism is redundantly actuated, the actuated joint set can be described by

$$\boldsymbol{\theta}_A = [\boldsymbol{\theta}_s^T \quad \boldsymbol{\theta}_a^T]^T \tag{27}$$

where $\boldsymbol{\theta}_s$ denotes a subset of the dependent (or redundantly actuated) joint set $\boldsymbol{\theta}_p$.

The static relationship between $\boldsymbol{T}_u$ and $\boldsymbol{T}_A$ is given by

$$\boldsymbol{T}_u = [G_u^A]^T\boldsymbol{T}_A \tag{28}$$

where $[G_u^A]$ is equivalent to

$$[G_u^a] = [G_a^A][G_u^a]. \tag{29}$$

In (29), $[G_a^A]$ is a subset of $[G_a^\phi]$ define in (13) and $[G_u^a]$ is the inverse of $[G_a^u]$ defined in (17). Since $[G_u^A]$ is not a square matrix and the dimension of $\boldsymbol{T}_A$ is greater than that of $\boldsymbol{T}_u$, $\boldsymbol{T}_A$ has infinite solution for a given $\boldsymbol{T}_u$. In particular, we employ a minimum norm solution of $||\boldsymbol{T}_A||$.

The solution is given by

$$\boldsymbol{T}_A = ([G_u^A]^T)^+\boldsymbol{T}_u \tag{30}$$

where $([G_u^A]^T)^+$ given by

$$([G_u^A]^T)^+ = [G_u^A]([G_u^A]^T[G_u^A])^{-1} \tag{31}$$

denotes the pseudo-inverse of the matrix $([G_u^A]^T)$.

The limit on the driving force T_{An} at the nth actuated joint is given as

$$(T_{An})_{\min} = -T_{An}^A + T_{An}^G \tag{32}$$

and

$$(T_{An})_{\max} = T_{An}^A + T_{An}^G \tag{33}$$

where T_{An}^A is the actuation limit at the nth actuator and T_{An}^G is the gravity load at the nth actuated joint.

The relationship between T_{An} and $\boldsymbol{T}_u$ is obtained from (30) as

$$T_{An} = [G_A^u]_{(*,n)}^T\boldsymbol{T}_u \tag{34}$$

where $[G_A^u]$ is identical to $([G_u^A]^T)^+$, and $[G_A^u]_{(*,n)}$ denote the nth column vector of $[G_A^u]$.

Now, we want $\boldsymbol{T}_u$ which simultaneously satisfies the constraint equations (32) and (33) and minimize $||\boldsymbol{T}_u||^2$, defined as

$$||\boldsymbol{T}_u||^2 = \boldsymbol{T}_u^T[W]\boldsymbol{T}_u \tag{35}$$

where $[W] \equiv \text{diag}\{W_i\}$. Based on Lagrangian multiplier-based optimization method, the maximum allowable load for the nth joint is obtained as

$$(T_u)_{\max} = (T_{An})_{ext}([G_A^u]_{(*,n)}^T[W]^{-1}[G_A^u]_{(*,n)})^{-1/2} \tag{36}$$

where $(T_{An})_{ext}$ is given as

$$(T_{An})_{ext} = \min\{|(T_{An})_{\min}|, |(T_{An})_{\max}|\}. \tag{37}$$

The above results must be evaluated for all available actuators. The smallest value among all $(T_u)_{\max}^n$ is regarded as the maximum load handling capacity.

B. Simulation

It is recalled that two actuators are minimally required to control the five-bar finger mechanism. Here, we are concerned about where to locate the two actuators. In fact, 10 possible sets exist since there are five joints in the system. So far, the base joints have been preferred as the actuator location since dynamic effect due to the floating actuator can be ignored. However, the choice of the two base joints as the actuator location does not always assures the best kinematic characteristics such as manipulability and isotropy. Other set of the actuators may yield a better kinematic characteristics. Even, the dynamic effect due to the floating actuators can be discarded by using a belt system which connects the floating joint to another actuator located at the base. Therefore, we ignore the additional dynamic effect due to the floating actuators. However, in real application of belt-drive, there needs extra effort to compensate for friction or flexible dynamic characteristic of belts. Also, we do not consider gravity loads in the analysis of a planar five-bar mechanism for simplicity, though it can be easily included in our problem.

Initially, the kinematic and dynamic parameters of the system are given as

$$l_1 = l_3 = l_4 = l_5 = a = 0.1\text{ m}, \quad l_2 = 0.2\text{ m},$$
$$m_1 = m_3 = m_4 = 0.3\text{ kg}, \quad m_2 = 0.6\text{ kg} \tag{38}$$

and

$$I_{z1} = I_{z3} = I_{z4} = 0.00025\text{ kg}\cdot\text{m}^2,$$
$$I_{z2} = 0.002\text{ kg}\cdot\text{m}^2.$$

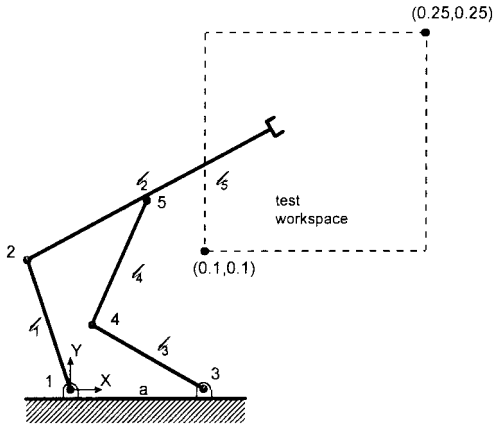

Fig. 4. Workspace of five-bar finger mechanism.

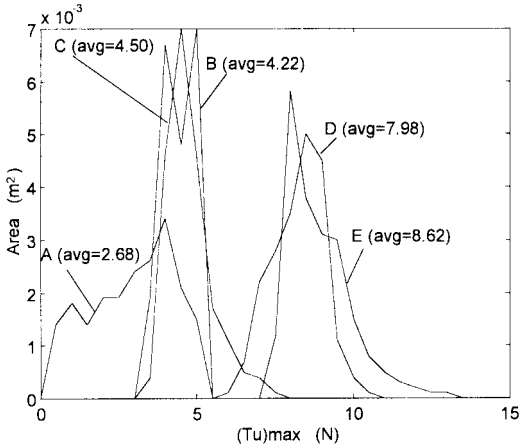

Fig. 5. Maximum load handling capacity.

In the simulation, we measure and compare the performance of the system in terms of maximum load handling capacity. The following three issues are to be investigated.

1) Where are the best locations for the minimum actuators (2)?
2) How does one additional actuator affect the performance and where to locate it?
3) How does more additional actuators affect the performance?.

First of all, we are concerned about where to locate the minimum actuators. Assume that the maximum actuator size is given by $-1 \leq T_{A_n} \leq 1$ (N · m) for each actuator. Among 10 possible minimum sets, we just compare the performances of two minimum sets $(\theta_1\ \theta_3)$ and $(\theta_1\ \theta_2)$. The desired workspace is given as $0.1 \leq x,\ y \leq 0.25$(m), as shown in Fig. 4. The curves A and B in Fig. 5 denote the distribution of maximum load handling capacity at the end-effector and it's averaged values for the minimum set $(\theta_1\ \theta_3)$ and the minimum set $(\theta_1\ \theta_2)$, respectively. The horizontal axis denotes the value of maximum load handling capacity and the vertical axis denotes the area occupied by each load handling capacity. The simulation result shows that the minimum set with one floating joint has greater load handling capacity in comparison with the maximum load handling capacity of the two base actuators. This result shows that choice of the two base joints as the actuator location does not always assures the best performance.

Secondly, our concern is about the performance enhancement due to one additional actuator. The curves, C and D represent the distribution of maximum load handling capacity at the end-effector and the average value, for the actuator set $(\theta_1\ \theta_2\ \theta_3)$ and the actuator set $(\theta_1\ \theta_2\ \theta_4)$, respectively. When we compare the load handling capacity of $(\theta_1\ \theta_3)$ with that of $(\theta_1\ \theta_2\ \theta_4)$, the load handling capacity of the latter is three-times of that of the former. Though there are many possible sets with one additional actuator, the above result addresses that one additional actuator greatly improves the performance of the system, and thus the location of the additional actuator is also significant.

Thirdly, the curve E of Fig. 5 denotes the distribution of maximum load handling capacity and the average value when employing the whole actuators. It is observed that the load handling capacity is not much improved in comparison with that of the curve D for the case of one additional actuator. Based on this analysis, we can conclude that one additional actuator rather than many redundant actuators plays an important role in improving the load handling capacity of the system.

Here, we discuss the reason why redundant actuation improves the load handling capacity. Different from usual serial robot structures, closed-chain mechanisms have several paths to the ground. Thus, structurally they can support large operational forces. They also have several potential input locations such as five-bar treated in this work. Thus, placement of redundant actuators on the joints imposes a kinematic dependence among actuators. This situation allows even distribution of the operational loads to the system actuators. Accordingly, the required operational load can be supported with small amount of actuation effort as compared to that of the minimum actuation. In other words, for the given actuator capacity, maximum allowable load handling capacity will be improved.

IV. Internal Force Applications

A. Feedforward Stiffness Modulation

In a state of static equilibrium, (13) can be described by

$$\boldsymbol{T}_a^* = [G_a^A]^T \boldsymbol{T}_A = 0. \tag{39}$$

Given a disturbance to the system under force equilibrium, a spring-like behavior occurs to the system. Assuming that the magnitude of $\boldsymbol{T}_A$ remains constant, the effective stiffness matrix $[K_{aa}]$ with respect to the independent coordinates is obtained by differentiating (39) with respect to the independent coordinate set ϕ_a [21]

$$[K_{aa}] = (-\boldsymbol{T}_A)^T \circ [H_{aa}^A]^T. \tag{40}$$

It has been known [21] that the effective stiffness matrix in the output position is given in terms of $[K_{aa}^*]$ as

$$[K_{uu}^*] = [G_u^a]^T [K_{aa}][G_u^a] \tag{41}$$

where $[G_u^a]$ is equivalent to the inverse of $[G_a^u]$. Substituting (40) into (41) yields

$$[K_{uu}^*] = [G_u^a]^T(-\boldsymbol{T}_A^T \circ [H_{aa}^A]^T)[G_u^a] \tag{42}$$

which is equivalently expressed as

$$[K_{uu}^*] = -\boldsymbol{T}_A^T \circ [H_{uu}^A] \tag{43}$$

where $\boldsymbol{T}_A$ satisfies the static equilibrium (39) and

$$[H_{uu}^A] = [G_u^a]^T[H_{aa}^A][G_u^a]. \tag{44}$$

An alternative form of (43) is given in a matrix form described by

$$\boldsymbol{K}_u = -[H_u^A]\boldsymbol{T}_A \tag{45}$$

where $\boldsymbol{K}_u$ consists of the upper diagonal elements of $[K_{uu}]$, and $[H_u^A]$ is also obtained by collecting the upper diagonal columns of the 3-D array $[H_{uu}^A]$, which are defined as follows:

$$\boldsymbol{K}_u = (K_{xx} \quad K_{xy} \quad K_{yy})^T \tag{46}$$

and

$$[H_u^A] = \begin{bmatrix} ([G_u^a]^T[H_{aa}^A][G_u^a])_{(*,1,1)} \\ ([G_u^a]^T[H_{aa}^A][G_u^a])_{(*,1,2)} \\ ([G_u^a]^T[H_{aa}^A][G_u^a])_{(*,2,2)} \end{bmatrix}. \tag{47}$$

B. Feedforward Frequency Modulation

Given a small displacement to the system in a state of static equilibrium ($\dot{\boldsymbol{u}} = 0$), the dynamic equation of the system is given, from (24), as

$$[I_{uu}^*]\delta\ddot{\boldsymbol{u}} = \boldsymbol{T}_u \tag{48}$$

where

$$\begin{aligned} \boldsymbol{T}_u &= \Delta([G_u^A]^T\boldsymbol{T}_A) \\ &= (\boldsymbol{T}_A^T \circ [H_{uu}^A]^T)\delta\mathbf{u}. \end{aligned} \tag{49}$$

The above equation is rearranged as

$$[I_{uu}^*]\delta\ddot{\mathbf{u}} + [K_{uu}]\delta\mathbf{u} = 0 \tag{50}$$

where $[K_{uu}]$ is the stiffness matrix given in (41). Premultiplying $[I_{uu}^*]^{-1}$ to both sides of (50) yields

$$\delta\ddot{\mathbf{u}} + [I_{uu}^*]^{-1}[K_{uu}]\delta\mathbf{u} = 0 \tag{51}$$

where the frequency matrix $[w_{uu}]$ is defined according to

$$\begin{aligned} [w_{uu}][w_{uu}]^T &= [I_{uu}^*]^{-1}[K_{uu}] \\ &= (-T_A)^T \circ ([I_{uu}^*]^{-1}[H_{uu}^A]). \end{aligned} \tag{52}$$

Assuming that the frequency matrix is diagonal, (52) can be written in a matrix form

$$\omega_u = [W_u^A]\boldsymbol{T}_A \tag{53}$$

where ω_u and $[W_u^A]$ are obtained in a similar way to (46) and (47)

$$\omega_u = (\omega_{xx}^2 \quad \omega_{xy}^2 \quad \omega_{yy}^2)^T \tag{54}$$

and

$$[W_u^A] = \begin{bmatrix} ([G_u^a]^T[W_{aa}^A][G_u^a])_{(*,1,1)} \\ ([G_u^a]^T[W_{aa}^A][G_u^a])_{(*,1,2)} \\ ([G_u^a]^T[W_{aa}^A][G_u^a])_{(*,2,2)} \end{bmatrix}. \tag{55}$$

C. Load Distribution Algorithms

Now, in order to modulate the desire K_u (or ω_u) in static equilibrium, a load distribution method is introduced in this section, Yi and Freeman [21] derived necessary conditions for stiffness modulation by antagonistic preloading in redundantly actuated systems (Appendix 2). According to those conditions, a planar closed-chain system having one closed-loop has two nonholonomic constraint equations, which allow modulation of the same number of stiffness elements. Since the dimension of the matrix $[K_{uu}]$ is 2×2, only two components out of k_{xx}, k_{xy}, and k_{yy} can be independently controlled with the remaining one controlled dependently. In regard of the number of actuators, at least, four actuators are necessary to control the motion in the x- and y-directions and the magnitudes of two stiffness elements. For instance, assume that only the magnitudes of k_{yy} and k_{xy} are to be controlled. Now, combine (39) and (45) in a matrix form, given by

$$\begin{bmatrix} [G_a^A]^T \\ -[H_u^A]^* \end{bmatrix}\boldsymbol{T}_A = \begin{bmatrix} 0 \\ \boldsymbol{K}_u^* \end{bmatrix} \tag{56}$$

where $[H_u^A]^*$ denotes a matrix consisting of the second and third rows of $[H_u^A]$ of (47) and $\boldsymbol{K}_u^*$ denotes the second and third elements of $\boldsymbol{K}_u$.

Then, the general solution of (56) is described by

$$\boldsymbol{T}_A = [G_{com}]^+\mathbf{a} + ([I] - [G_{com}]^+[G_{com}])\epsilon \tag{57}$$

where $[G_{com}]^+$ denotes a pseudo-inverse solution of $[G_{com}]$. $[G_{com}]$ and $\boldsymbol{a}$ are given as

$$[G_{com}] = \begin{bmatrix} [G_a^A]^T \\ -[H_u^A]^* \end{bmatrix} \tag{58}$$

and

$$\boldsymbol{a} = \begin{bmatrix} 0 \\ \omega_u \end{bmatrix}. \tag{59}$$

Also, the second-term of (57) represents a homogeneous solution which creates an internal loading which is independent of motion and stiffness or motion frequency modulated under static equilibrium. This internal loading can be utilized for additional subtasks. In order to modulate the motion frequency, replace $[H_u^A]^*$ and $\boldsymbol{K}_u^*$ in (56) with $[W_u^A]^*$ and ω_u^*.

D. Simulation

In simulation, the magnitudes of k_{yy} and k_{xy} are to be controlled as 500 N/m and 0 N/m, respectively, at the position of $(x, y) = (0.1, 0.1)$ m. The actuator load $\boldsymbol{T}_A$ is decided such that the desired stiffness can be modulated. In order to test the spring effect created by antagonistic redundant actuation, an initial displacement from the equlibrium position is given to the y direction by 1 cm, which initiates the acceleration of the system. A fourth-order Runge–Kutta integration algorithm is used to obtain the dynamic reponse of the system. Fig. 6 demonstrates the vibration phenomenon of the system along the y-direction. A small vibration occurs in the x-direction. This is due to the dynamic coupling between the two translational directions in the output space.

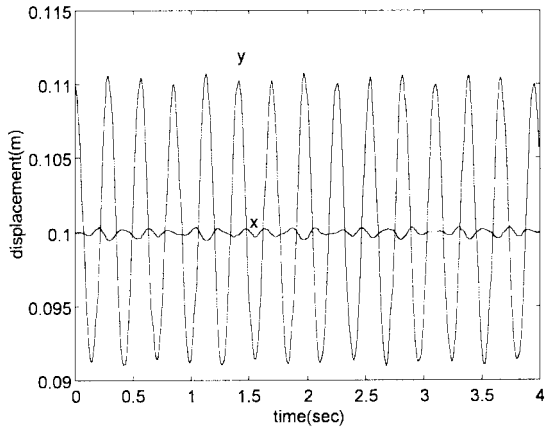

Fig. 6. Spring effect ($K_{yy} = 500$ N/m).

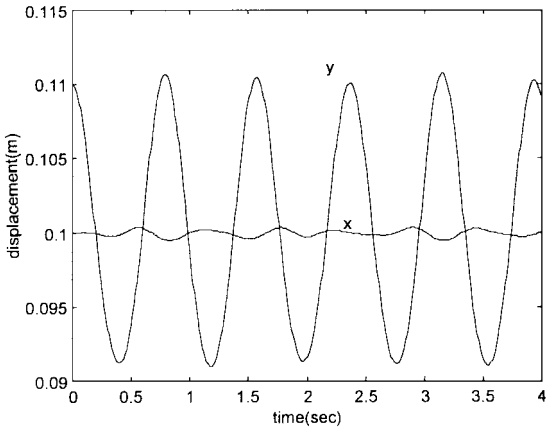

Fig. 8. Frequency control ($\omega = 8$ rad/s).

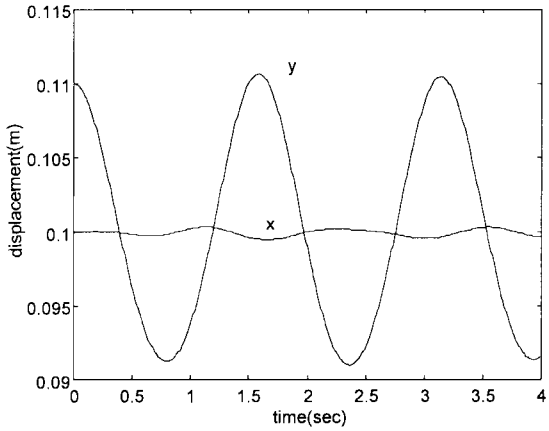

Fig. 7. Frequency control ($\omega = 4$ rad/s).

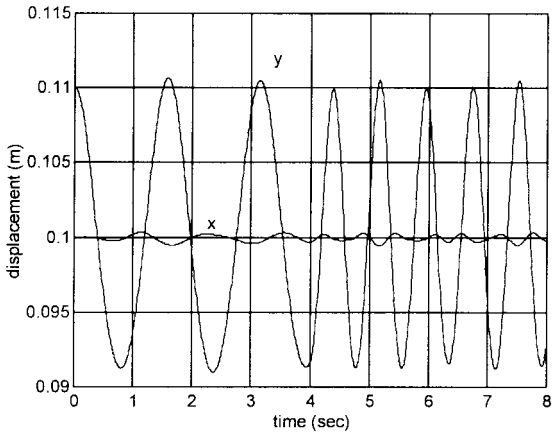

Fig. 9. End-effector motion with frequency modulation from $\omega = 4$ rad/s to $\omega = 8$ rad/s.

In the meanwhile, for the purpose of controling the natural frequency of the system, we employ the frequency modulation algorithm introduced in Section IV-B. The initial displacement from the equilibrium position is given the same. The actuator load $\boldsymbol{T}_A$ is decided such that ω_{xy} becomes zero and ω_{yy} is modulated as a certain value. Figs. 7 and 8 show the vibration behaviors when the natural frequencies in the y-direction are modulated as 4 rad/sec and 8 rad/sec, respectively, by using redundant actuation. Since the frequency of the system is related to the period of vibration, described by

$$T = \frac{2\pi}{\omega} \tag{60}$$

T can be estimated for each case. Just as expected, T of Fig. 7 is two times of that of Fig. 8. The proposed frequency modulator has the following features:

1) Actively adjustable frequency modulation: The oscillation of the five-bar finger mechanism with respect to a desired position can be achieved by activating the system actuators such that the system has the desired frequency characteristics at the equilibrium position, with the initial position of the end-point being deviated from the equilibrium position by the amount of the desired amplitude of oscillation. Fig. 9 shows the vibration response in which the motion frequency ω_{xy} is modulated as zero steadily, but the motion frequency ω_{yy} along the y-direction shifts from 4 rad/s to 8 rad/s. This can be achieved by switching the system actuation efforts for the initial motion frequency to those for the second motion frequency.

2) Actively adjustable equilibrium position: Suppose that we calculate the actuator efforts for two equilibrium positions about which harmonic oscillation will be generated according to the planned motion frequency. Assume that the system is undergoing harmonic oscillation about the initial equilibrium position. During the motion, change of the equilibrium position can be made by abruptly switching the actuator efforts for the initial position to those for the goal position. Fig. 10 shows the shifting of the equilibrium position from $(0.1\ 0.1)$ m to $(0.1\ 0.11)$ m with the same motion frequency of 8 rad/s. Also, Fig. 11 shows the transition of the equilibrium position from $(0.1\ 0.1)$ m to $(0.1\ 0.105)$ m with the same motion frqeuency of 8 rad/s. Note that for both cases the magnitudes of oscillation have been changed. This is because the inertial property for each equilibrium position is different from that of the original equilibrium position, and thus the resulting motions show different amplitude of oscillation. It is here remarked that a kinematically redundant structure such as a six-bar mechanism (this configuration can be achieved by adding up one joint and one link in the first chain of the five-bar finger mechanism) can be possibly employed to modulate

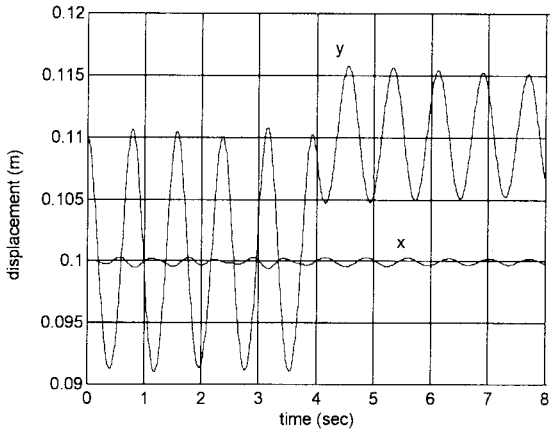

Fig. 10. End-effector motion with the equilibrium position shift from (0.1, 0.1) to (0.1, 0.11).

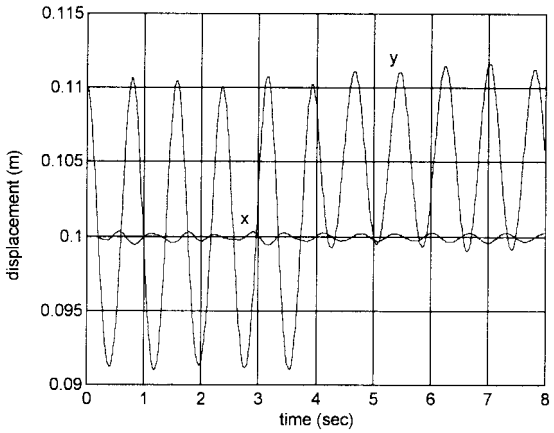

Fig. 11. End-effector motion with the equilibrium position shift from (0.1, 0.1) to (0.1, 0.105).

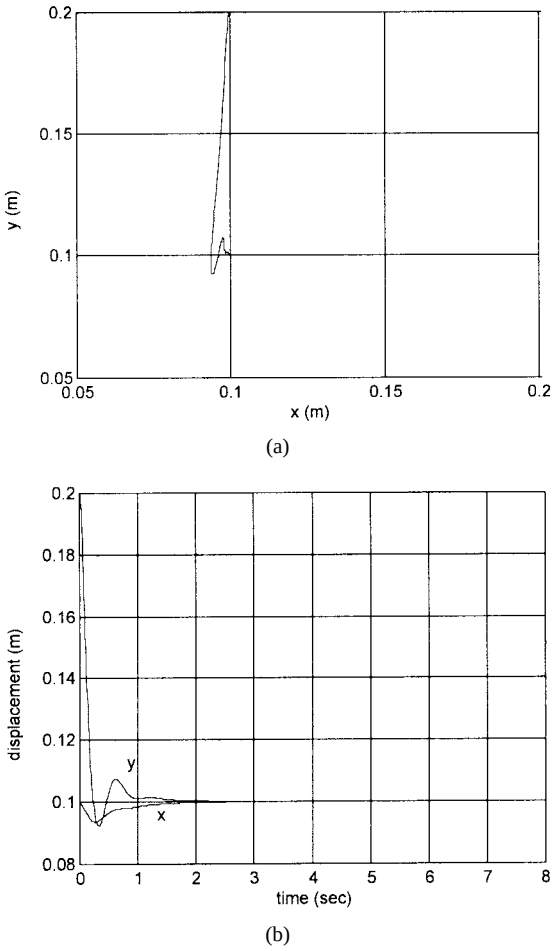

Fig. 12. Virtual trajectory generation. (a) Time versus displacement plot (b) x versus y plot.

the same motion frequency of the system in a more active manner, even in the case of transition of the equilibrium position, since the same inertia property can be possibly modulated by the self-motion using the kinematic redundancy of the kinematically redundant structure.

The proposed motion frequency is a local property and it is controlled in an open-loop fashion. Therefore, stability issue is important specially in changing the equilibrium position. Too much traveling distance between the two equlibrium position may drive the system to unstable situation. Sensitivity analysis for the mapping matrix given in (58) will be useful to anticipate the stability of the system. We consider a sensitivity measure which is defined as the variation of the singular values of the mapping matrix with respect to the equilibrium position (i.e., x and y). This kind of index has been employed to measure the sensitivity of Jacobians of redundant robot manipulators. Small sensitivity measure implies that the frequency content of the system does not change too much around the equilibrium positions, which enable the system to shift from one to another equilibrium position in a stable fashion. In real design problem of frequency modulator, minimization of this index should be considered as one of the design objectives for stable operation.

3) Virtual trajectory planning: The spring-like property coupled with the inertia of the human body defines the property of frequency content. Thus, a certain frequency content of the system behavior is directly converted to the spring-like property. It has been mentioned [6] that modulation of the spring-like property could be employed to produce movement of the system. The production of the movement can be accomplished by a progressive movement of the equilibrium position, which is called a virtual trajectory. Fig. 12 illustrates a virtual trajectory, which has been achieved by changing the equilibrium position fromm (0.1 0.2) to (0.1 0.1). The stiffness characteristics at both position are given the same as $k_{xy} = 0$ and $k_{yy} = 100$ N/m. An equivalent frequency content can be calculated from (53). In order to suppress the vibration about the global position, a damping effect is included as

$$[D] = \begin{bmatrix} -65 & 0 \\ 0 & -65 \end{bmatrix} \text{N} \cdot \text{sec}. \tag{61}$$

The principle significance of the virtual trajectory is that it implies a drastic reduction in the computational effort required to obtain the inverse dynamics for movement generation of robot manipulators [6]. For a better steady state response, a continuous movement of the equilibrium position may be desirable.

It is remarked that stiffness and frequency modulations will be useful in several complex assembly applications. For example, consider a two-fingered hands grasping a common object. Each finger is made as our proposed five-bar finger mechanism. It is expected that a certain assembly work such as peg-in-hole problem can be easily performed by inducing vibration to the grasped object. This vibration can be created by a synchronized motion frequency modulation of the two fingered hands. Besides assembly works, the applications of stiffness and motion frequency modulation will be diverse, which will be a future research topic.

V. Conclusion

A redundantly actuated five-bar finger mechanism is studied in this work. This configuration would be not only free from the friction effect occurring in tendon-driven fingers, but also increase the payload of the finger due to redundant actuators as well as provide chances of applying several beneficial subtasks using internal loading. We illustrated that judicial choice of one additional actuator greatly enhanced the maximum load handling capacity of the system in comparison to those of nonredundant case and more than two redundant actuation case. The results can be applied to general closed-chain systems having redundant actuators. Furthermore, stiffness and frequency control algorithms utilizing internal loading created by redundant actuation of the system were introduced. The concept of the frequency modulation is considered fairly new.

Our future study will be focused on experimental verification of the proposed algorithms and application of the proposed five-bar finger mechanism to manipulation and control of multi-fingered hands.

Appendix I

Operator "$\circ$" is called as *the generalized scalar dot product* [2] and is defined as follows: let A and B represent a $p \times q$ matrix and a 3-D $q \times (m \times n)$ array. The resulting $p \times (m \times m)$ array C is obtained as

$$C_{(p,i,j)} = [A \circ B]_{(p,i,j)} = \sum_{k=1}^{q} A_{(p,k)} B_{(k,i,j)}.$$

Appendix II

A. Necessary Conditions for Full Stiffness Generation in Redundantly Actuated Parallel Mechanisms [21]

A closed-chain mechanism is capable of full stiffness generation only if it satisfies

$$J_a \geq D + M$$

where

- D number of independent stiffness elements ($= M(M+1)/2$);
- M degree of freedom (system mobility);
- J_a number of active joints;

and

$$NC = (IC - LC) \geq D$$

where

- IC number of independent constraint equations;
- NC number of dependent nonlinear constraint equations;
- LC number of independent linear constraint equations.

References

[1] P. A. Spence, *Basic Human Anatomy*. New York: Benjamin/Cummings, 1986.

[2] R. A. Freeman and D. Tesar, "Dynamic modeling of serial and parallel mechanisms/robotic systems, Part I—Methodology, Part II—Applications," in *Proc. 20th ASME Mech. Conf.*, 1988, vol. 15-3, pp. 7–27.

[3] H. J. Kang, B.-J. Yi, W. Cho, and R. A. Freeman, "Constraint-embedding approaches for general closed-chain system dynamic in terms of a minimum coordinate set," in *Proc. 1990 ASME Biennial Mech. Conf.*, Chicago, IL, 1990, vol. 24, pp. 125–132.

[4] M. Thomas, H. C. Yuan-Chou, and D. Tesar, "Optimal actuator sizing for robotic manipulators based on local dynamic criteria," *ASME J. Mech., Transm., Automat. Design*, vol. 107, pp. 163–169, 1985.

[5] H. Asada and K. Youcep-Toumi, "Analysis and design of a direct drive arm with a five-bar link parallel drive mechanism," *ASME J. Dyn. Syst., Meas., Contr.*, vol. 106, no. 3, 1982.

[6] N. Hogan, "Impedance control: An approach to manipulation: Part I—Theory, Part II: Implementation, Part III—Applications," *J. Dyn. Syst., Meas., Contr.*, vol. 107, pp. 1–24, 1985.

[7] V. J. Kumar and K. Waldron, "Force distribution in walking vehicles," in *Proc. 20th Biennial Mech. Conf.*, 1988, vol. 15-3, pp. 473–480.

[8] M. E. Pittelkau, "Adaptive load sharing force control for two arm manipulator," in *Proc. IEEE Conf. Robot. Automat.*, 1988, pp. 498–503.

[9] Y. F. Zheng and J. Y. S. Luh, "Optimal load distribution for two industrial robots handling a single object," in *Proc. IEEE Conf. Robot. Automat.*, 1988, pp. 344–349.

[10] A. N. Meyer and J. Angeles, "Force optimization in redundantly actuated closed kinematic chains," in *Proc. IEEE Conf. Robot. Automat.*, 1989, pp. 951–956.

[11] Y. Nakamura and M. Ghodoussi, "Dynamic computation of closed-link robot mechanisms with nonredundant and redundant actuators," *IEEE J. Robot. Automat.*, vol. 5, pp. 294–302, June 1989.

[12] M. A. Nahon, and J. Angeles, "Force optimization in redundantly-actuated closed kinematic chains," in *Proc. IEEE Robot. Automat. Conf.*, 1989, pp. 951–956.

[13] V. J. Kumar and J. Gardner, "Kinematics of redundantly actuated closed chain," *IEEE J. Robot. Automat.*, vol. 6, pp. 269–273, Apr. 1990.

[14] R. Kurz and W. Hayward, "Multiple-goal kinematic optimization of a parallel spherical mechanism with actuator redundancy," *IEEE J. Robot. Automat.*, vol. 8, pp. 644–651, Oct. 1992.

[15] B.-J. Yi and R. A. Freeman, "Feedforward spring-like impedance modulation in human arm models," in *Proc. IEEE Robot. Automat. Conf.*, 1995, pp. 3121–3128.

[16] A. S. Deo and I. D. Walker, "Dynamics and control methods for cooperating manipulators with rolling contact," in *Proc. IEEE Conf. Robot. Automat.*, 1995, pp. 1509–1516.

[17] W. Kwon and B. H. Lee, "Optimal load distribution of multiple cooperating robots using nonlinear programming dual method," in *Proc. IEEE Robot. Automat.*, 1996, pp. 2408–2413.

[18] L. Yun-Hui and X. Yangsheng, "Cooperating of multiple manipulators with passive joints," in *Proc. IEEE Conf. Robot. Automat.*, 1997, pp. 1478–1483.

[19] I. D. Walker, R. A. Freeman, and S. I. Marcus, "Internal object loading for multiple cooperating robot manipulators," in *Proc. IEEE Conf. Robot. Automat.*, 1989, pp. 606–611.

[20] B.-J. Yi and R. A. Freeman, "Synthesis of actively adjustable springs by antagonistic redundant actuation," *Trans. ASME J. Dyn. Syst., Meas., Contr.*, vol. 114, pp. 454–461, 1992.

[21] ———, "Geometric analysis of antagonistic stiffness in redundantly actuated parallel mechanisms," *Special Issues on Parallel Closed-Chain Mech., J. Robot. Syst.*, vol. 10, pp. 581–603, 1993.

[22] D. Cox and D. Tesar, "Multi-level criteria for dual-arm robotic operations," in *Proc. IEEE Conf. Robot. Automat.*, 1994, pp. 1243–1249.

[23] R. G. Bonitz and T. C. Hsia, "Robust internal force based impedance control for cooperating manipulators—Theory and experiments," in *Proc. IEEE Conf. Robot. Automat.*, 1996, pp. 622–628.

[24] H. J. Yeo, I. H. Suh, B. J. Yi, and S. R. Oh, "A single closed-loop kinematic chain approach for a hybrid control of two cooperating arms with a passive joint: An application to sawing task," *IEEE Trans. J. Robot. Automat.*, vol. 15, pp. 141–151, Feb. 1999.
[25] B.-J. Yi, S. R., Oh, and I. H. Suh, "Analysis of a five-bar finger mechanism having redundant actuators with applications to stiffness and frequency modulation," in *Proc. IEEE Robot. Automat. Conf.*, 1997, pp. 759–765.
[26] B.-J. Yi, S.-R. Oh, I. H. Suh, and B.-J. You, "Synthesis of actively adjustable frequency modulators via redundant actuation: The case for a five-bar finger mechanism," in *Proc. IEEE/RSJ Int. Conf. Intell. Robot. Syst. (IROS)*, 1997, pp. 1098–1104.
[27] D. Sreevijayan, "On the design of fault-tolerant robotic manipulator systems," M.S. thesis, Dept. Mech. Eng., Univ. Texas, Austin, 1992.

Byung-Ju Yi (M'89) received the B.S. degree from the Department of Mechanical Engineering, Hanyang University, Seoul, Korea in 1984, and the M.S. and Ph.D. degrees from the Department of Mechanical Engineering, University of Texas at Austin, in 1986 and 1991, respectively.

From January 1991 to August 1992, he was a Post-Doctoral Fellow with the Robotics Group, University of Texas at Austin. From September 1992 to February 1995, he was an Assistant Professor in Department of Mechanical and Control Engineering, Korea Institute of Technology and Education (KITE), Chonan, Chungnam, Korea. In March 1995, he joined Hanyang University, Ansan, Kyungki-Do, Korea as an Assistant Professor in the Department of Control and Instrumentation Engineering. Currently, he is an Associate Professor with the School of Electrical Engineering and Computer Science, Hanyang University. His research interests include design, control, and application of multiple arms, parallel manipulator, micromanipulator, haptic device, and anthropomorphic manipulator systems.

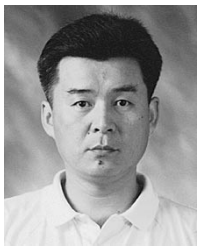

Sang-Rok Oh (S'80–M'91) received the B.S. degree in electronic engineering from Seoul National University, Seoul, Korea, in 1980, and the M.S. and Ph.D. degrees in electrical and electronic engineering from the Korea Advanced Institute of Science and Technology (KAIST), Daeduk, Korea, in 1982 and 1987, respectively.

He worked as a Research Associate at the Systems Control Laboratory, KAIST, for ten months in 1987, conducting the design and implementation of multiprocessor-based automatic assembly machine for micro electronic components and robotic control system for multilegged locomotion. In 1988, he joined the Korea Institute of Science and Technology (KIST), and is a Principal Research Engineer at the Intelligent System Control Research Center, KIST. He was a Visiting Scientist at the T. J. Watson Research Center, IBM, Yorktown Heights, NY, from 1991 to 1992, conducting precision assembly using the magnetically levitated robot twist. He also worked as a Visiting Scientist at the Mechanical Engineering Laboratory, Tsukuba, Japan, for three months in 1995, investigating the area of mobile manipulation system. His research interests include intelligent control of robot manipulators, mobile manipulation, multifingered robotic hand, and service robots.

Dr. Oh is a member of the Korea Institute of Electrical Engineering, the Korea Fuzzy Logic and Intelligent System Society, and the Institute of Control, Automation, and System Engineering, Korea.

Il Hong Suh (M'89) was born in Seoul, Korea. He received the B.S. degree in electronics engineering from Seoul National University in 1977 and the M.S. and Ph.D. degrees in electrical engineering from the Korea Institute of Science and Technology (KAIST), Seoul, in 1979 and 1982, respectively.

From 1982 to 1985, he was a Senior Research Engineer at the Technical Center of Daewoo Heavy Industries, Ltd., Inchon, Korea, where he was involved in the research works in machine vision and the development of the Daewoo NOVA10 robot controller. From 1985 to 1986, he was with the Systems Control Laboratory, KAIST, as a part-time Research Fellow for an automation-related Korea National Project. In 1987, he was a Visiting Research Fellow at the Robotics Division, CRIM, University of Michigan, Ann Arbor. Since 1985, he has been with the Department of Electronics Engineering, Hanyang University, Korea, where he is a Professor. His research interests include sensor based control of robot manipulators, coordination of multiple robot arms, and robot control intelligent control involving fuzzy logics, and neural networks.